

Supplementary Materials

Table S1. Summary of N-doped CNT and proposed mechanistical pathway.

Carbocatalyst	Pollutant	N-doping (%)	O-Functional Groups	Key active sites for Radical and Non-Radical Pathway	
N-SWCNT	Phenol	0.80	1.15	Radical pathway - $\text{SO}_4^{\cdot-}$, $\cdot\text{OH}$ -C=O more active site Non-radical Pathway - Electron-transfer reaction from N dopants to PMS - graphitic N act as effective active site	[33]
N-CNT	Phenol	1.51-7.34	--	Non-radical – electron-transfer regime via NCNT-PMS* complex	[34]
N-MWCNT	Phenol	0.88	3.30	Pyridinic N and Pyrrolic N dopants are much more active sites than O-functional groups	[35]
N-SWCNT	Phenol	0.80	1.15	PMS activation by N-SWCNT contributes non-radical pathway	[36]
FeC@NCNT	Phenol	1.82	--	Radical pathway - $\text{SO}_4^{\cdot-}$, $\cdot\text{OH}$, $\text{O}_2^{\cdot-}$ Non-radical Pathway ${}^1\text{O}_2$	[37]
N-CNT	Bisphenol A	--	--	Non-radical (${}^1\text{O}_2$) process is dominants BPA degradation and - $\text{SO}_4^{\cdot-}$, $\cdot\text{OH}$ and $\text{O}_2^{\cdot-}$ only play auxiliary roles	[57]

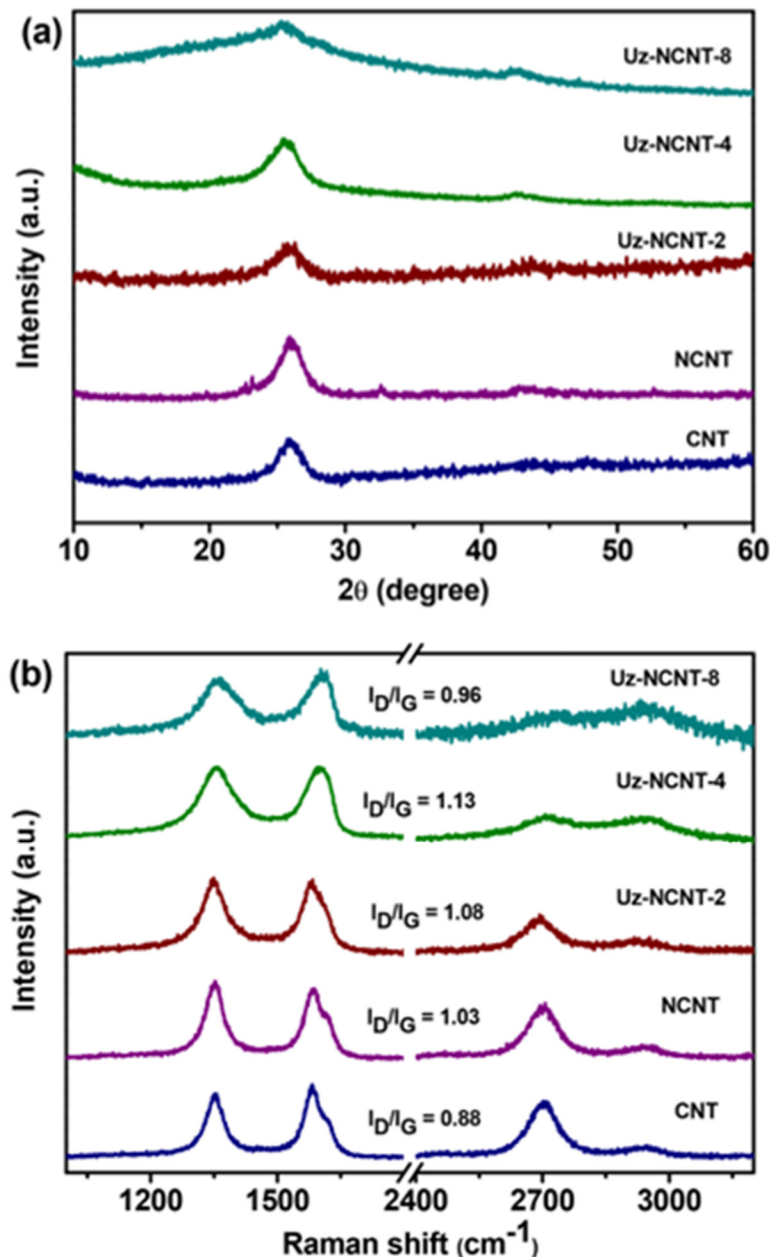


Figure S1. (a) XRD patterns and (b) Raman spectrum of CNT, NCNT and unzipped NCNTs.

Table S2. Details of Raman spectra and I_D/I_G ratio.

Carbocatalysts	D band	I _D	G band	I _G	2D band	I _D /I _G	Number of Graphene Layer
CNT	1351	947	1585	1080	2703	0.8768	multi-layer
NCNT	1351	1037	1585	1006	2716	1.0303	multi-layer
Uz-NCNT-2	1347	956	1591	880	2698	1.0863	multi-layer
Uz-NCNT-4	1353	2837	1612	2508	2712	1.1311	multi-layer
Uz-NCNT-8	1359	1108	1608	1118	2732	0.9606	multi-layer

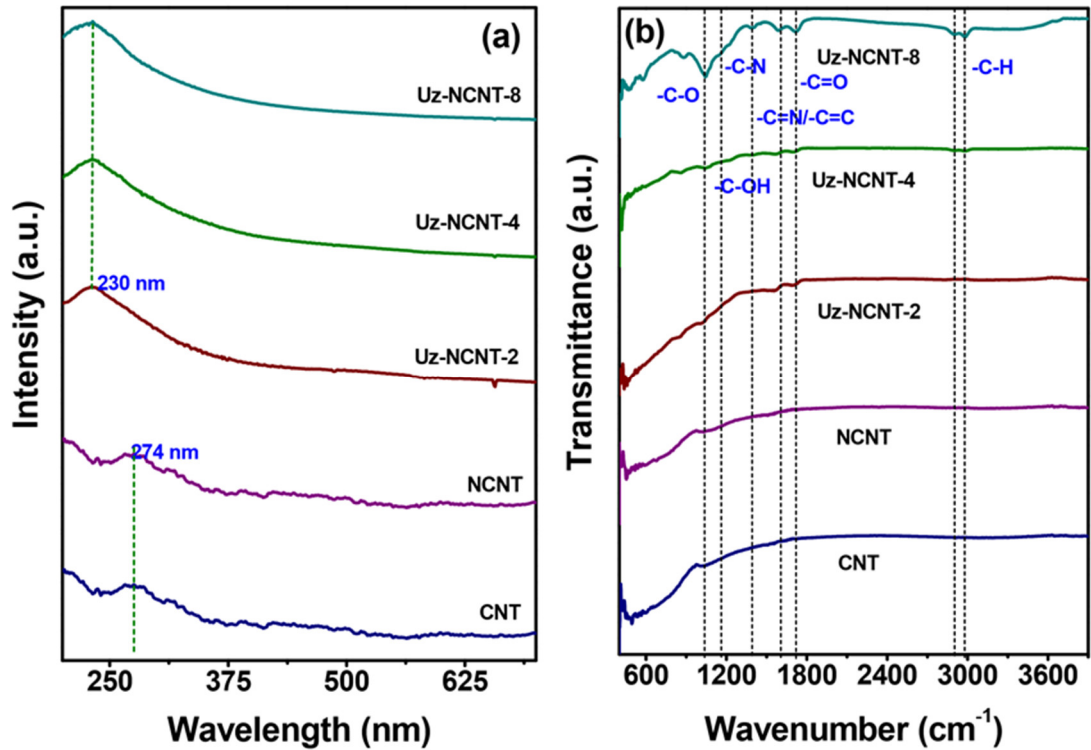


Figure S2. (a) UV-visible spectrum and (b) FT-IR spectrum of CNT, NCNT and unzipped NCNTs.

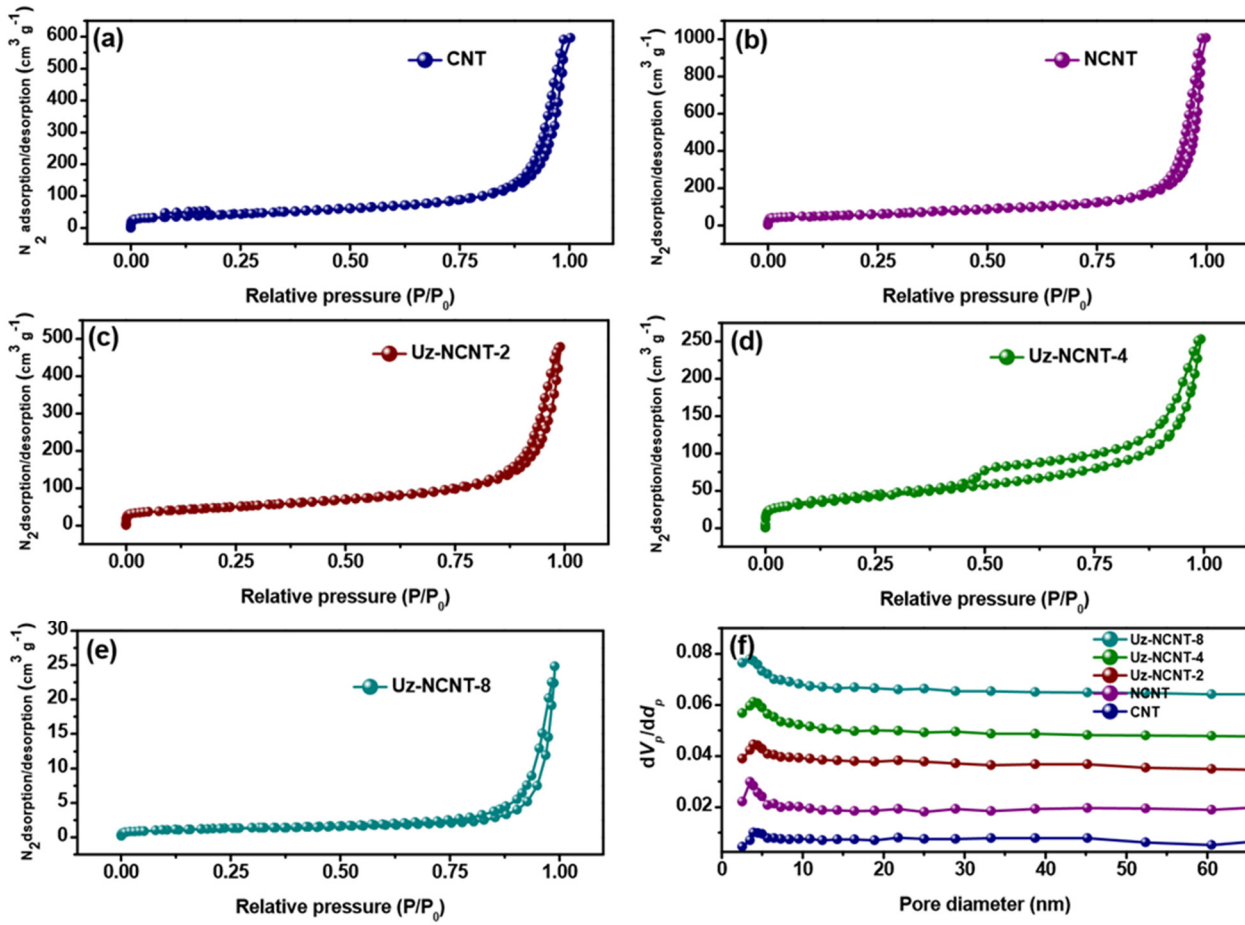


Figure S3. BET N_2 adsorption/desorption profile of (a) CNT, (b) NCNT, (c) Uz-NCNT-2, (d) Uz-NCNT-4, (e) Uz-NCNT-8 and (f) BJH pore diameter.

Table S3. BET surface area and BJH pore diameter of derived carbocatalysts.

Carbocatalyst	Specific Surface area ($\text{m}^2 \text{ g}^{-1}$)	Total Pore Volume ($\text{cm}^3 \text{ g}^{-1}$)	Average Pore Diameter (nm)
CNT	206.41	1.455	26.607
N-MWCNT	207.06	1.4043	27.79
Uz-NCNT-2	163.04	0.752	17.604
Uz-NCNT-4	140.72	0.373	10.603
Uz-NCNT-8	4.4125	0.03839	34.801

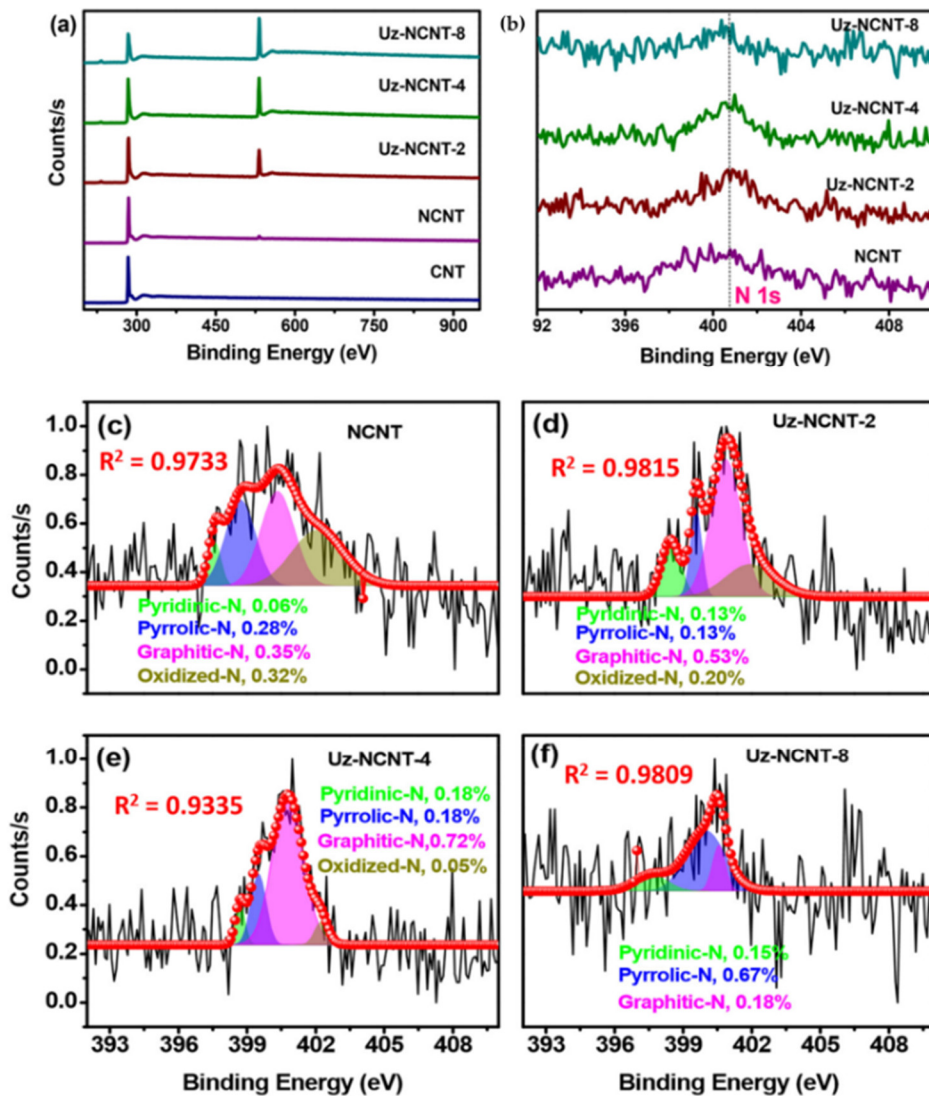


Figure S4. (a) XPS survey spectrum, (b) N 1s core-level spectra, deconvoluted N 1s core-level spectra of (c) NCNT, (d) Uz-NCNT-2, (e) Uz-NCNT-4 and (f) Uz-NCNT-8.

Table S4. Atomic percentage of N-dopants in carbocatalysts was determined from N 1s spectra.

N-dopants	Area	Peak Center (eV)	Width	Height	Fraction (at.%)
NCNT					
Pyridinic N	0.124	397.604	0.541	0.182	0.058
Pyrrolic N	0.594	398.714	1.331	0.356	0.281
Substitutional N	0.732	400.333	1.491	0.392	0.346
Oxidized N	0.667	402.088	2.299	0.231	0.315
Total area	2.116				1.000
Uz-NCNT-2					
Pyridinic N	0.238	398.465	0.813	0.234	0.133
Pyrrolic N	0.229	399.566	0.504	0.363	0.128
Substitutional N	0.952	400.873	1.339	0.568	0.533
Oxidized N	0.366	401.930	2.163	0.135	0.205
Total area	1.785				1.000
Uz-NCNT-4					
Pyridinic N	0.085	398.696	0.408	0.166	0.059
Pyrrolic N	0.254	399.498	0.684	0.296	0.175
Substitutional N	1.035	400.789	1.337	0.618	0.716
Oxidized N	0.073	402.235	0.607	0.095	0.050
Total area	1.446				1.000
Uz-NCNT-8					
Pyridinic N	0.123	397.629	1.463	0.067	0.153
Pyrrolic N	0.538	399.989	1.718	0.250	0.671
Substitutional N	0.142	400.564	0.590	0.192	0.176
Total area	0.803				1.000

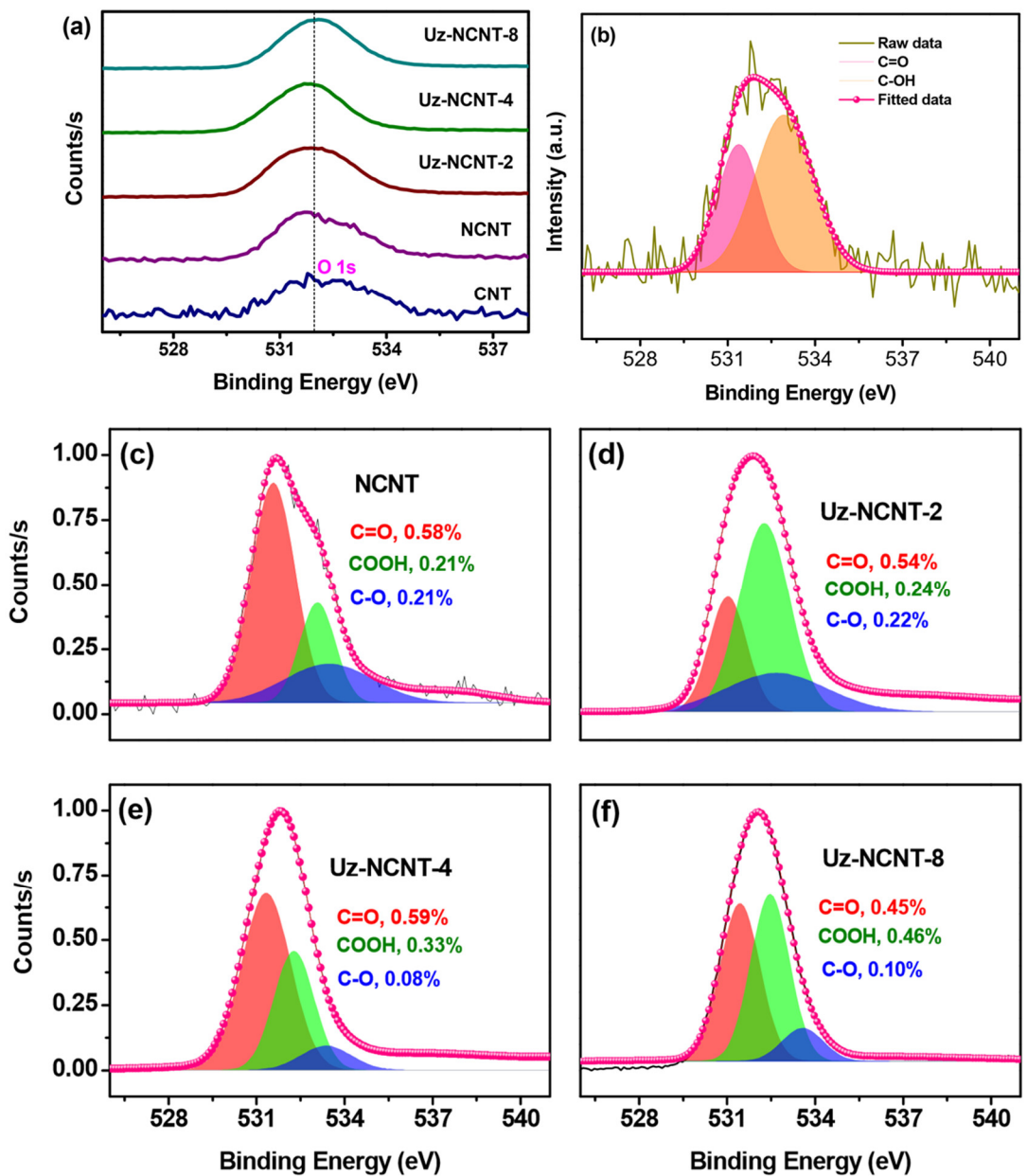


Figure S5. (a) C 1s spectra, and deconvoluted O 1s core-level spectra of (b) NCNT, (c) Uz-NCNT-2, (d) Uz-NCNT-4 and (e) Uz-NCNT-8 and (f) Uz-NCNT-8.

Table S5. Atomic percentage of oxygen containing functional groups in carbocatalysts was determined from O 1s spectra.

O-groups	Area	Center	Width	Height	Fraction (%)
CNT					
C-O	1.47	532.92	2.03	0.58	0.63
C=O	0.88	531.38	1.49	0.47	0.37
Total area	2.35				1.00
NCNT					
C-O	0.57	533.65	3.04	0.15	0.21
C=O	1.60	531.57	1.50	0.85	0.58
COOH	0.59	533.71	1.22	0.39	0.21
Total area	2.76				1.00
Uz-NCNT-2					

C-O	0.65	533.08	3.46	0.15	0.22
C=O	1.58	532.57	1.72	0.73	0.54
COOH	0.72	531.53	1.29	0.45	0.24
Total area	2.95				1.00
Uz-NCNT-4					
C-O	0.21	533.57	1.75	0.09	0.08
C=O	1.43	531.43	1.68	0.68	0.59
COOH	0.79	532.47	1.38	0.46	0.33
Total area	2.43				1.00
Uz-NCNT-8					
C-O	0.23	533.58	1.42	0.13	0.10
C=O	1.04	531.54	1.37	0.61	0.45
COOH	1.07	532.47	1.33	0.64	0.46
Total area	2.338				1.000

Table S6. Summary of key active sites in carbocatalyst/PMS activation for ACP degradation.

Structure-activity	Active N-groups	Correlation Co-efficient (R^2)	Active O-groups	Correlation Co-efficient (R^2)
	Pyridinic N	0.9219	-C=O	0.9699
<i>Structure</i> — k_1 (ACP)	Graphitic N	0.8891	-C-O	0.9364 (downtrend)
<i>Structure</i> — k_1 (PMS)	Graphitic N	0.7014	-C=O	0.9775

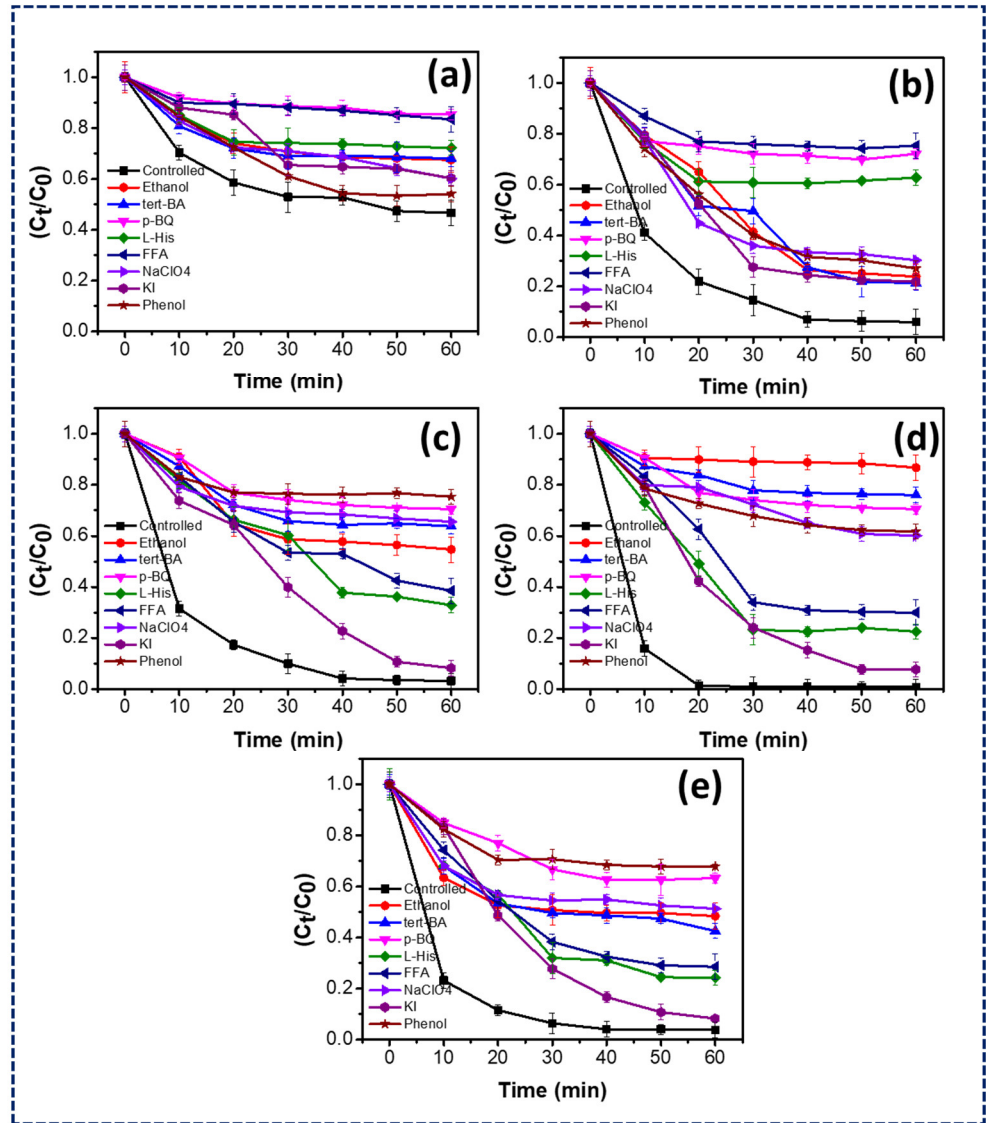


Figure S6. (a) Effect of various chemical quenchers on normalized ACP concentration at (a) CNT/PMS, (b) NCNT/PMS, (c) Uz-NCNT-2/PMS, (d) Uz-NCNT-4/PMS and (e) Uz-NCNT-8/PMS systems. Quenching studies were performed with $C_{ACP} = 10 \text{ mg L}^{-1}$, $C_{Catalyst} = 100 \text{ mg L}^{-1}$, $C_{PMS} = 0.5 \text{ mM}$, $C_{Ethanol} \text{ or } C_{tert-BA} = C_{p-BQ} = 500 \text{ mM}$ or $C_{FFA} = C_{L-His} = C_{NaClO_4} = C_{phenol} = C_{KI} = 50 \text{ mM}$.

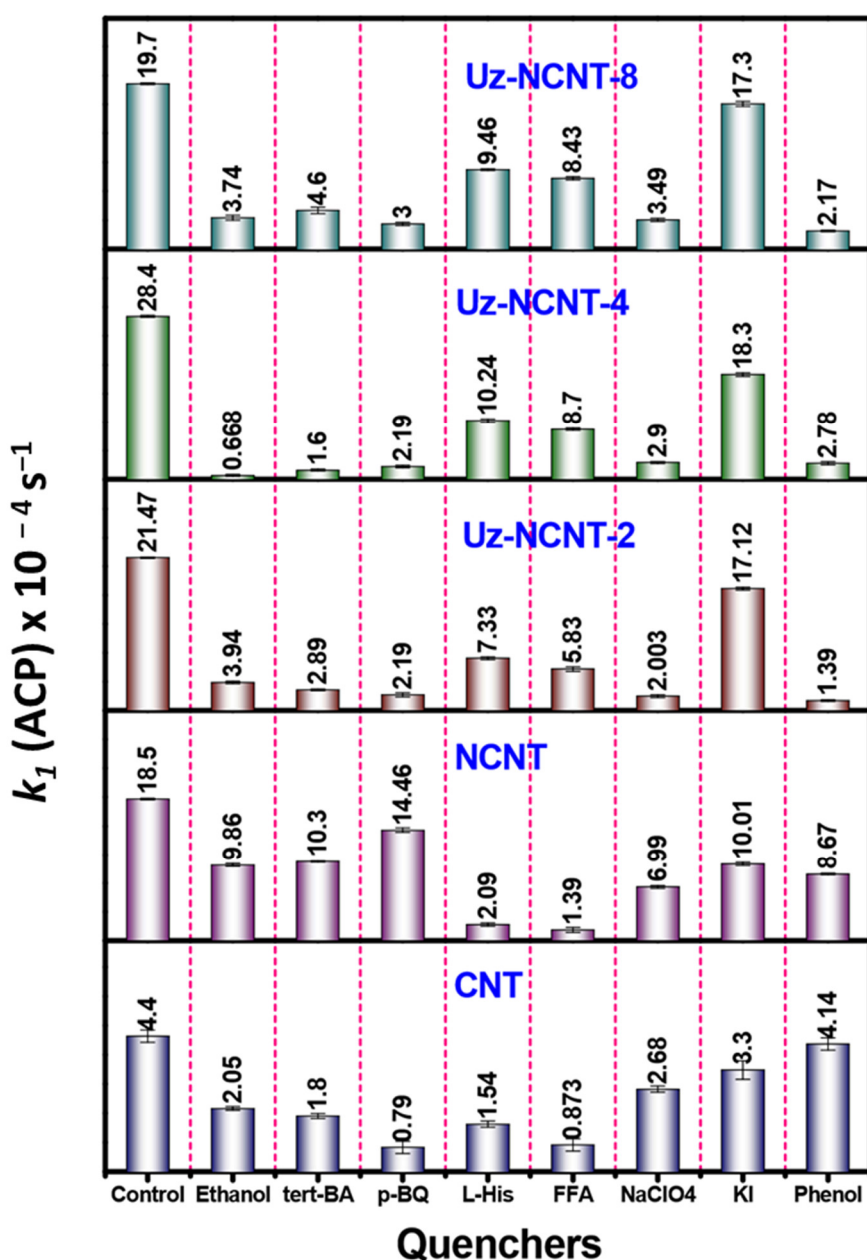


Figure S7. Impact of chemical scavengers on k_1 (ACP) under different catalytic systems. Quenching studies were carried out at $C_{\text{ACP}} = 10 \text{ mg L}^{-1}$, $C_{\text{Catalyst}} = 100 \text{ mg L}^{-1}$, $C_{\text{PMs}} = 0.5 \text{ mM}$, $C_{\text{Ethanol}} \text{ or } C_{\text{tert-BA}} = C_{\text{p-BQ}} = 500 \text{ mM}$ or $C_{\text{FFA}} = C_{\text{L-His}} = C_{\text{NaClO}_4} = C_{\text{phenol}} = C_{\text{KI}} = 50 \text{ mM}$.

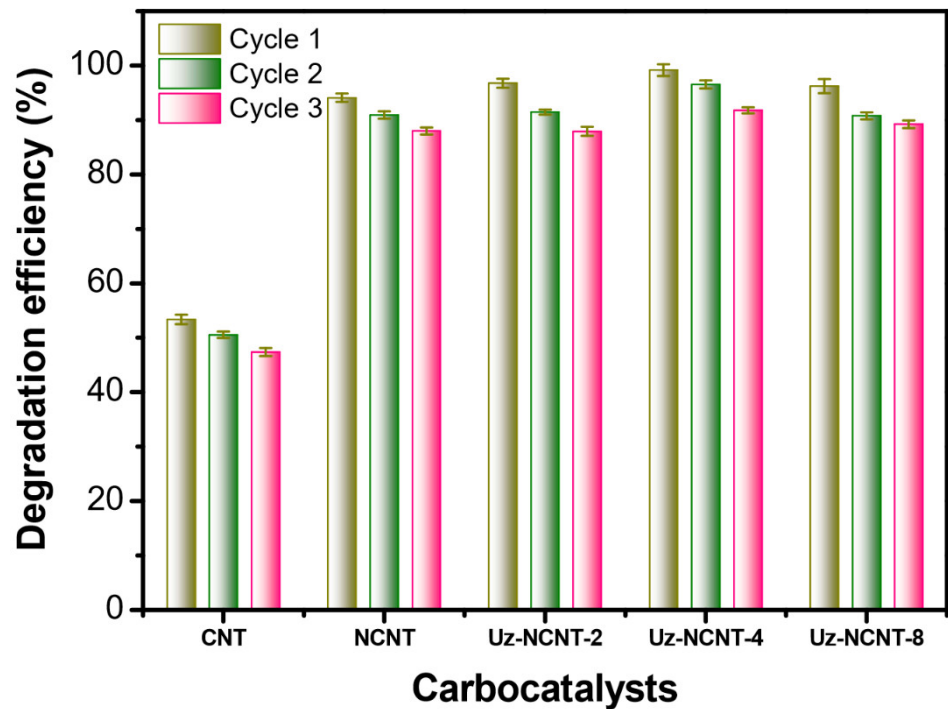


Figure S8. ACP degradation efficiency by reusability test in three consecutive runs. Experimental conditions $C_{ACP} = 10 \text{ mg L}^{-1}$, $C_{Catalyst} = 100 \text{ mg L}^{-1}$, $C_{PMS} = 0.5 \text{ mM}$ and $pH_0 = 7 \pm 0.3$.